AMERICAN SOCIETY FOR MICROBIOLOGY | Antimicrobial Agents and Chemotherapy

Molecule Targeting Glucosyltransferase Inhibits *Streptococcus mutans* Biofilm Formation and Virulence

Zhi Ren,[a] Tao Cui,[b] Jumei Zeng,[c] Lulu Chen,[a] Wenling Zhang,[a] Xin Xu,[a] Lei Cheng,[a] Mingyun Li,[a] Jiyao Li,[a] Xuedong Zhou,[a] Yuqing Li[a]

State Key Laboratory of Oral Diseases, West China Hospital of Stomatology, Sichuan University, Chengdu, People's Republic of China[a]; State Key Laboratory of Agricultural Microbiology, Center for Proteomics Research, College of Life Science and Technology, Huazhong Agricultural University, Wuhan, People's Republic of China[b]; Department of Structural Biology, Key Laboratory of Applied and Environmental Microbiology, Chengdu Institute of Biology, Chinese Academy of Sciences, Chengdu, People's Republic of China[c]

Dental plaque biofilms are responsible for numerous chronic oral infections and cause a severe health burden. Many of these infections cannot be eliminated, as the bacteria in the biofilms are resistant to the host's immune defenses and antibiotics. There is a critical need to develop new strategies to control biofilm-based infections. Biofilm formation in *Streptococcus mutans* is promoted by major virulence factors known as glucosyltransferases (Gtfs), which synthesize adhesive extracellular polysaccharides (EPS). The current study was designed to identify novel molecules that target Gtfs, thereby inhibiting *S. mutans* biofilm formation and having the potential to prevent dental caries. Structure-based virtual screening of approximately 150,000 commercially available compounds against the crystal structure of the glucosyltransferase domain of the GtfC protein from *S. mutans* resulted in the identification of a quinoxaline derivative, 2-(4-methoxyphenyl)-*N*-(3-{[2-(4-methoxyphenyl)ethyl]imino}-1,4-dihydro-2-quinoxalinylidene)ethanamine, as a potential Gtf inhibitor. *In vitro* assays showed that the compound was capable of inhibiting EPS synthesis and biofilm formation in *S. mutans* by selectively antagonizing Gtfs instead of by killing the bacteria directly. Moreover, the *in vivo* anti-caries efficacy of the compound was evaluated in a rat model. We found that the compound significantly reduced the incidence and severity of smooth and sulcal-surface caries *in vivo* with a concomitant reduction in the percentage of *S. mutans* in the animals' dental plaque ($P < 0.05$). Taken together, these results represent the first description of a compound that targets Gtfs and that has the capacity to inhibit biofilm formation and the cariogenicity of *S. mutans*.

Dental caries is one of the most prevalent human diseases across all age groups (1). It is estimated that over 90% of the world's population will experience dental caries at least once during their lifetime (2). If left untreated, dental caries ultimately leads to pain, pulpal infection, and even tooth loss, and the impact of oral health on general health has already drawn great concern (3). Dental caries arises from chronic biofilms containing cariogenic microbes that break down fermentable carbohydrates (primarily sucrose) into organic acids that cause demineralization and destruction of tooth tissue (1).

Among cariogenic microbes, *Streptococcus mutans* is regarded as the major etiological pathogen (4). *S. mutans* is acidogenic and acid tolerant, can utilize sucrose to synthesize extracellular polysaccharides (EPS) through glucosyltransferases (Gtfs), and can adhere to glucan-coated tooth surfaces, which make up the three most important virulence factors involved in the pathogenesis of dental caries. Reports have shown that individuals with dental plaque containing low levels of *S. mutans* are more resistant to exogenous colonization with other cariogenic pathogens and are more resistant to dental caries in the long run (5–7). In addition, low levels of *S. mutans* contribute to the maintenance of healthy dentition, while progressively increasing levels of *S. mutans* are closely related to the development of caries in children (8).

Currently, cariogenic dental biofilms are eradicated mainly by nonspecific mechanical removal (brushing and flossing) or by treatment with broad-spectrum antibiotics (chlorhexidine). Apart from the extensive use of fluoride, a number of new anticariogenic methods have started to draw attention. Derivatives of natural products, such as cranberry constituents (9), fractions of barley coffee (10), and tea catechins (11, 12), have been shown to have inhibitory effects against *S. mutans* biofilm formation. In addition, numerous small molecules, including *tt*-farnesol (12), chitosan, 7-epiclusianone (13), and apigenin (14), have been characterized and have been shown to have antibiofilm activity. Other potential anticariogenic methods include sugar substitutes (15), probiotic strains (16), and arginine (17). However, few of these treatments have been proven to confer selectivity against *S. mutans* biofilms. In recent years, targeted antimicrobials capable of selectively eliminating *S. mutans* have been designed to achieve targeted killing with a minimal effect on other oral microbes (18–20), opening up alternative methods to prevent caries without disturbing the ecological balance between pathogens and commensal bacteria in the oral cavity.

Dental biofilms develop after initial microbial attachment on the tooth surface followed by formation and stabilization of highly structured microcolonies, which are formed in a polysaccharide-

Received 19 April 2015 **Returned for modification** 20 July 2015
Accepted 30 September 2015

Accepted manuscript posted online 19 October 2015

Citation Ren Z, Cui T, Zeng J, Chen L, Zhang W, Xu X, Cheng L, Li M, Li J, Zhou X, Li Y. 2016. Molecule targeting glucosyltransferase inhibits *Streptococcus mutans* biofilm formation and virulence. Antimicrob Agents Chemother 60:126–135. doi:10.1128/AAC.00919-15.

Address correspondence to Yuqing Li, liyuqing@scu.edu.cn.

Z.R. and T.C. contributed equally to this article.

Supplemental material for this article may be found at http://dx.doi.org/10.1128/AAC.00919-15.

rich extracellular matrix (21). *S. mutans* is a key contributor to this extracellular matrix due to the production of glucans by three Gtfs (22): GtfB, which synthesizes mainly insoluble glucans with α(1-3) glycosidic linkages; GtfC, which synthesizes a mixture of insoluble and soluble glucans; and GtfD, which synthesizes predominantly soluble glucans with α(1-6) linkages (23). GtfB and GtfC have been associated with the initial microbial adherence and the structural stability of the extracellular matrix, and they have also been shown to be essential for *S. mutans* virulence in a rat caries model (24–26). In particular, GtfC has been shown to possess the greatest affinity for the hydroxyapatite surface, followed by GtfB and then GtfD (26).

Recently, the crystal structure of GtfC, a glycoside hydrolase (GH) family 70 glucansucrase, was determined, and many novel structural features were revealed (27). It is the only crystallographic structure to date that has been precisely identified among the glucansucrases encoded by *S. mutans*. Considering the importance of GtfC in EPS synthesis, its role in *S. mutans* biofilm formation, and, consequently, its cariogenic capacity, the structure of GtfC provides extremely useful clues for the design of novel structure-based enzyme inhibitors that may be further developed into therapeutic drugs for the prevention of dental caries.

Structure-based virtual screening of large compound libraries is one of the most advanced approaches to identify new antibacterial agents but has been rarely applied in the field of dental research. In this study, we report the discovery of a novel *S. mutans* Gtf inhibitor through the use of the structure-based virtual screening of approximately 150,000 compounds from commercially available databases. Virtual screening for Gtf inhibitors resulted in the identification of 51 chemically diverse compounds, which were then tested against *S. mutans* UA159. Of the 51 potential inhibitors, we identified one compound that is a potent enzyme antagonist with the capacity to inhibit the biofilm formation and cariogenicity of *S. mutans*.

MATERIALS AND METHODS

***In silico* inhibitor screen.** UCSF DOCK (version 6.4) (28) was used for an *in silico* docking-based virtual screen. The compound library was obtained from the ZINC database (29). The three-dimensional structure of GtfC (Protein Data Bank [PDB] accession number 3AIC) was obtained from the PDB database (30). Following the DOCK 6 protocol, the protein structure was processed step by step, which included the addition of hydrogen atoms and charge information, the generation of structure surface data, the generation of sphere data, the selection of representative spheres of the binding pocket (spheres that, within a 6.0 space around a carbose, were selected in this study), the generation of the grid box, and the calculation of energy grid data. Then, the predicted binding score with GtfC of each molecule in the compound library was calculated with DOCK 6 and ranked. Compounds used for *in vitro* assays were purchased from Specs Company (Delft, Netherlands).

Visualization and protein-ligand contact analysis. The structural figures were prepared using Chimera (31). The protein-ligand interactions were analyzed using LigPlot+ (32).

Chemicals, test bacteria, and growth conditions. The compound 2-(4-methoxyphenyl)-*N*-(3-{[2-(4-methoxyphenyl)ethyl]imino}-1,4-dihydro-2-quinoxalinylidene)ethanamine was purchased from Specs Company, and a stock solution of the compound was prepared in dimethyl sulfoxide (DMSO; Sigma, Taufkirchen, Germany). *S. mutans* UA159, *Streptococcus sanguinis* ATCC 10556, and *Streptococcus gordonii* ATCC 10558 were commercially obtained from the American Type Culture Collection (ATCC). The *gtf* mutants (Δ*gtfB*, Δ*gtfC*, and Δ*gtfB* Δ*gtfC*) of *S. mutans* were kindly provided by Robert A. Burne (Department of Oral Biology, University of Florida, Gainesville, FL). All of the bacteria were grown routinely in brain heart infusion (BHI) broth (Difco, Sparks, MD, USA) in an anaerobic chamber (10% H_2, 5% CO_2, and 85% N_2; Thermo Fisher Scientific, Inc., Waltham, MA, USA) at 37°C. Inoculum for the experiment was adjusted to 1×10^7 CFU/ml and diluted 1:10 (1:4 for *S. sanguinis* to obtain reproducible and compatible biofilms) in the growth culture for all experiments. For biofilm growth, 1% sucrose (Sigma) was added to BHI broth (BHIS). For all biofilm assays, the final concentration of DMSO in the wells was 1%. To ensure DMSO had no effect on the experimental set-up, control wells with no DMSO and 1% DMSO were present in each assay.

Planktonic growth assays. The effect of the compound on planktonic *S. mutans* growth was tested using a 96-well cell culture plate. Overnight cultures of *S. mutans* UA159 were inoculated into BHI broth containing 10 μg/ml and 5 μg/ml of the compound and were incubated at 37°C for 16 h. The optical density at 595 nm (OD_{595}) was recorded hourly using a microplate reader (BioTek, Winooski, VT, USA) as previously described (33). A medium containing 250 μg/ml ampicillin (Sigma) was used as a positive control. Medium-only wells (without bacteria) served as blanks.

Biofilm formation assays. To test the inhibitory effect of the compound on *S. mutans* biofilm formation, overnight cultures of *S. mutans* UA159 and the *gtf* mutants (Δ*gtfB*, Δ*gtfC*, and Δ*gtfB* Δ*gtf*C) were inoculated into wells of a 48-well cell culture plate containing BHIS as previously described with several modifications (33). To examine the effects of the compound on biofilm formation by other oral bacteria and more than one species, *S. sanguinis* and *S. gordonii* were inoculated into BHIS with 10 μg/ml compound separately or simultaneously with *S. mutans*. Plates were incubated anaerobically at 37°C for 24 h. Spent culture medium was decanted, and the plates were washed twice with sterile phosphate-buffered saline (PBS) to remove planktonic and loosely adherent cells. Adherent cells from the biofilm were resuspended by vigorous pipetting and vortexing and were serially diluted 10^6-fold through 10^8-fold and plated onto BHI agar plates. The agar plate was incubated anaerobically at 37°C for 48 h before the cells were enumerated to determine the number of CFU.

Mature biofilm assay. The effect of the compound on mature biofilms was assessed by following the protocol of Stepanovic et al. (34) with some modifications. Briefly, BHIS was inoculated in a flat-bottom 48-well cell culture plate, and overnight cultures of *S. mutans* UA159 were added and were then incubated anaerobically for 24 h at 37°C to form mature biofilms. After 24 h, the medium was carefully aspirated, and new medium with the compound at concentrations of either 5 or 10 μg/ml was added to the wells and incubated at 37°C for 72 h under anaerobic conditions. At 24, 48, and 72 h after inoculation, the medium was decanted, and the plates were washed twice with sterile PBS to remove planktonic and loosely adherent cells. Adherent cells from the biofilm were resuspended by vigorous pipetting and vortexing and were serially diluted 10^6-fold through 10^8-fold and plated onto BHI agar plates. The plates were incubated anaerobically at 37°C for 48 h before the cells were enumerated to determine the number of CFU.

Quantitative determination of water-insoluble EPS. The inhibitory effect of the compound on water-insoluble EPS synthesis was confirmed. Briefly, overnight cultures of *S. mutans* UA159 and the *gtf* mutant strain were anaerobically cultured in flat-bottom 24-well cell culture plates for 48 h at 37°C in BHIS with either 5 or 10 μg/ml of the compound. Blank wells received BHIS only. After 48 h of incubation, the culture fluid was carefully removed and replaced with 2 ml sterile PBS. Cells in each well were resuspended by vigorous pipetting and vortexing, and 1 ml of each suspension was transferred to a sterile 1.5-ml centrifuge tube. The suspension was centrifuged at 6,000 × *g* for 10 min at 4°C. The supernatant was discarded, and the pellet was resuspended and washed 3 times with sterile PBS to ensure all of the water-soluble extracellular polysaccharides were removed (14). Water-insoluble extracellular polysaccharides were extracted from the sample according to the procedure of Koo et al. using 1.0 M NaOH with agitation for 2 h at 37°C (9). The concentration of alkali-

soluble carbohydrate was determined in the supernatant using the anthrone-sulfuric method. Briefly, the alkali-soluble carbohydrate solution was mixed with three volumes of anthrone-sulfuric acid reagent and was heated in a water bath at 95°C for 5 min until the reaction was complete. The solution was then allowed to cool to room temperature, and its absorbance was measured in a 96-well cell culture plate at 625 nm using a microplate reader (BioTek).

SEM. The effect of the compound on the *S. mutans* biofilm structure and the EPS production was observed by scanning electron microscopy (SEM). An overnight culture of *S. mutans* UA159 was inoculated into BHIS with 10 μg/ml compound on glass coverslips and placed in a 24-well cell culture plate. After 24 h of incubation, the biofilms were rinsed three times with sterile PBS to remove planktonic and loosely adherent cells and were fixed overnight with 2.5% glutaraldehyde at 4°C. The coverslips were rinsed once with PBS and were dehydrated in an absolute ethanol series. Samples were coated with gold before being observed under SEM (FEI, Hillsboro, OR, USA).

CLSM analysis of biofilms. An overnight culture of *S. mutans* UA159 was inoculated into BHIS with 10 μg/ml compound on glass coverslips and was anaerobically placed in a 12-well culture plate for 12, 24, 48, or 72 h. The architecture of the biofilms was observed by *in situ* labeling of bacterial cells and EPS as described previously (35). Alexa Fluor 647-labeled dextran conjugate (1 μM; Life Technologies, Grand Island, NY, USA) was added to the culture medium (BHIS) before inoculation with an overnight culture of *S. mutans* UA159. After incubation under anaerobic conditions for 12, 24, 48, or 72 h, the medium was decanted and the coverslips were washed twice with sterile PBS to remove planktonic and loosely bound cells; after this, the biofilms were labeled with 2.5 μM SYTO 9 green fluorescent nucleic acid stain (Life Technologies). Confocal imaging was performed using a Leica DM IRE2 confocal laser scanning microscope (CLSM; Leica, Wetzlar, Germany) with a 63× oil immersion objective. The image collection gates were set at 655 to 690 nm for Alexa Fluor 647 and at 495 to 515 nm for SYTO 9. During imaging, amplifier gain (1.0), detector gain (500 V), and offset (0%) were kept constant. Z sections were used to record the thickness of the biofilm, and each biofilm was scanned at five randomly selected positions. The three-dimensional architecture of the biofilms was visualized using Amira 5.0.2 (Mercury Computer Systems Inc., Chelmsford, MA, USA). COMSTAT image-processing software (36) was used to analyze the confocal image stacks and to calculate the biomass (covering percentage) of EPS and bacterial cells as previously described (35).

Adhesion force measurement by AFM. Atomic force microscopy (AFM) was used to analyze the adhesion force of *S. mutans* biofilm EPS in the presence and absence of the compound as described previously (37). Briefly, *S. mutans* UA159 biofilms were grown on sterile glass coverslips in BHIS supplemented with 5 or 10 μg/ml of the compound in 12-well culture plates. After 24 h of incubation, the biofilms were rinsed three times with sterile PBS to remove planktonic and loosely adherent cells. Biofilm adhesion was measured immediately after the final PBS rinse via atomic force microscopy (Shimadzu SPM-9700) in contact mode and was immersed in PBS (pH 7.2) at room temperature (20°C). The resulting force-distance curves were generated by moving the cantilever tip toward the biofilm, pressing against the biofilm surface, and retracting the tip slowly. About 50 force-distance curves were obtained at five different biofilm regions for each sample. Adhesion force was calculated by analyzing the final rupture events revealed on the curves.

Zymogram assays. The effect of the compound on the activities of GtfB, GtfC, and GtfD was determined by zymogram assays as described previously (38) with several modifications. Briefly, overnight cultures of *S. mutans* UA159 and the *gtf* mutants (Δ*gtfB*, Δ*gtfC*, and Δ*gtfB* Δ*gtf*C) were grown anaerobically in BHI broth treated with 10 μg/ml compound in a sterile 15-ml centrifuge tube for 5 h to an OD_{595} of 0.5 (mid-logarithmic phase). A parallel group treated with 1% DMSO served as a control. Bacterial cells were removed from the culture by centrifuging twice at 4°C (6,000 × *g* for 10 min). The supernatant was dialyzed at 4°C against 0.02 M sodium phosphate buffer at a pH of 6.8 and containing 10 μM phenylmethylsulfonyl fluoride (PMSF; Sigma) and was followed by dialysis against 0.2 mM sodium phosphate containing 10 μM PMSF. Samples were concentrated 100-fold using a 50-kDa centrifugal filter device (Millipore, Billerica, MA, USA) at 4°C, and 20 μl of each concentrated sample was resuspended in 2× loading buffer (1:1) and was applied to two sodium dodecyl sulfate (SDS)-6% polyacrylamide gels. Activity of the Gtfs was analyzed in simultaneously run duplicate SDS-polyacrylamide gel electrophoreses (SDS-PAGE) at 4°C using the Mini-Protean II system (Bio-Rad, Hercules, CA, USA). One gel was stained for total protein detection using Coomassie blue R-250 (Sigma) while the other gel was used for the zymogram assay. For zymogram analysis, after electrophoretic separation, the gel was washed three times for 10 min with renaturing buffer containing 2.5% Triton X-100 (Sigma), and this was followed by incubation for 18 h at 37°C in 0.2 M sodium phosphate buffer (pH 6.5) containing 5% sucrose and 0.2% dextran T70 (Sigma). Following the incubation period, the gel was washed with distilled water at 4°C for 10 min to stop the reaction. Digital images of the white, opaque glucan bands synthesized by the Gtfs were captured using a black background to enhance visibility.

***gtf* gene expression.** Quantitative reverse transcriptase PCR (qRT-PCR) was used to determine the effects of the compound on the expression of *gtfB*, *gtfC*, and *gtfD* mRNAs. An overnight culture of *S. mutans* UA159 was grown in BHI with 10 μg/ml compound to the late logarithmic phase. Total bacterial RNA isolation, purification, and cDNA reverse transcription were performed as described previously (39). Briefly, bacterial cells were harvested by centrifugation at 4°C (6,000 × *g* for 10 min) and were immediately stabilized with an RNAprotect bacterial reagent (Qiagen, Valencia, CA, USA). Bacterial cells were pelleted and resuspended in 100 μl of lysis buffer (20 mM Tris-HCl, 3 mM EDTA, 20 mg/ml lysozyme, and 60 mAU/ml proteinase K at pH 8.0) and were incubated at 37°C with gentle agitation for 20 min, after which the lysate was sonicated using a cup horn (Thermo Fisher Scientific) on ice for 2 cycles of ultrasonication for 60 s. The RNAs were purified with an RNeasy minikit (Qiagen). A First-Strand cDNA synthesis kit with random hexamer primers (TaKaRa, Shiga, Japan) was used to perform reverse transcription. qRT-PCR was performed on the Bio-Rad CFX96 system (Bio-Rad). All primers used are listed in Table S1 in the supplemental material. The reaction mixture (25 μl) contained 1× SYBR green PCR master mix (TaKaRa), template cDNA, and forward and reverse primers (10 mM each). Thermal cycling conditions were designated as follows: initial denaturation at 95°C for 30 s followed by 40 cycles of 95°C for 15 s and 60°C for 30 s. An additional step, from 95°C for 15 s to 60°C for 1 min (0.05°C s^{-1}), was performed to establish a melting curve. Threshold cycle values (C_T) were determined, and the data were analyzed by Bio-Rad CFX manager software (version 2.0) according to the $2^{-\Delta\Delta CT}$ method.

Animal studies. A rat model was used to determine the anti-caries activity of the compound *in vivo* as previously described with some modifications (40). Twenty-five female specific-pathogen-free (SPF) Sprague-Dawley rats aged 17 days and weighing 60 ± 5 g were purchased from Dashuo Inc. (Chengdu, China) and were infected with an overnight culture of *S. mutans* UA159 by oral lavage daily at the age of 19, 20, and 21 days (40, 41). The rats were fed diet no. 2000 (56% sucrose; Dashuo Inc.) and 5% sucrose water *ad libitum* (13, 40). At 22 days old, the infection was checked, and experimental rats were randomized into 5 groups with their teeth routinely treated using a sterile hair brush once daily. The groups consisted of the following: compound (10 μg/ml) (group 1), compound (5 μg/ml) (group 2), 250 μg/ml of fluoride (as positive control) (group 3), 1% DMSO (as vehicle control) (group 4), and deionized water (as negative control) (group 5). The experiment proceeded for 5 weeks, and all rats were weighed twice a week for the first 2 weeks and then weekly for the remainder of the experiment. Their physical appearance was routinely noted. At the completion of the fifth week of treatment, all animals were sacrificed by CO_2 asphyxiation. The left jaw was aseptically removed and sonicated in 5.0 ml of 154 mM sterile PBS. The suspensions were plated on

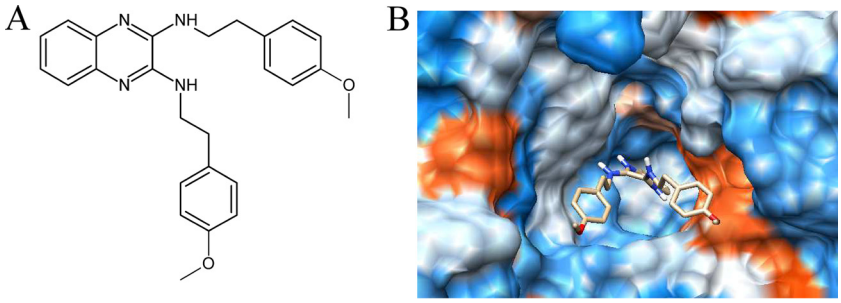

FIG 1 Chemical structure and molecular docking analysis of the compound identified in this study. (A) Chemical structure of the compound identified in this study. (B) Docking of 2-(4-methoxyphenyl)-*N*-(3-{[2-(4-methoxyphenyl)ethyl]imino}-1,4-dihydro-2-quinoxalinylidene)ethanamine on GtfC surface.

mitis salivarius agar (Difco) plus bacitracin (Sigma) to estimate the *S. mutans* population and on BHI agar plus 5% sheep blood to determine the total cultivable flora (37). After removal of flesh from the jaws, the teeth were stained for caries scoring by means of Larson's modification of Keyes' system (42). The determination of the caries score was blinded by codification of the jaws and was done by one experienced examiner. This study was reviewed and approved by the West China School of Stomatology Ethics Committee (WCCSSIRB-D-2014-013; Sichuan University, Chengdu, China).

Statistical analyses. For the *in vitro* studies, all experiments were performed at least in triplicate and reproduced three separate times. Statistical analyses of the data were performed with SPSS software (version 21.0 for Windows; SPSS Inc., Chicago, IL, USA) using analysis of variance (ANOVA), and a *post hoc* Tukey test was used for the comparison of multiple means. For the animal experiments, smooth- and sulcal-surface caries scores were expressed as proportions of their maximum possible values (124 and 56, respectively). The data were then subjected to ANOVA in the Tukey-Kramer honest standard deviation (HSD) test for all pairs. The level of significance was set at 5% ($P < 0.05$).

RESULTS

***In silico* structure-based screen for EPS inhibitors.** The glucosyltransferases of *S. mutans* play an essential role in the etiology and pathogenesis of dental caries. Therefore, the discovery of inhibitors of *S. mutans* Gtfs may facilitate the development of drugs that prevent dental caries. Gtfs catalyze the formation of glucans from sucrose via transglucosylation reactions, and finding small-molecule compounds that bind to the substrate binding pocket may interfere with the function of these enzymes. To address this, we performed molecule-docking-based virtual screening to identify potential small-molecule inhibitors of the substrate binding pocket of GtfC from *S. mutans*. In total, we screened ~150,000 small molecules against the substrate-binding site of GtfC. The predicted binding scores of each molecule within the GtfC substrate-binding site were sorted to select molecules with high binding potential. The top hits were expected to competitively bind the substrate-binding site of GtfC and, thus, inhibit glucan synthesis and biofilm formation. We identified 51 lead compounds and further screened these molecules for their inhibitory activities on EPS synthesis *in vitro* by utilizing a high-throughput anthrone-sulfuric acid method (see Fig. S1 in the supplemental material). Through this process, we identified a novel Gtf inhibitor, 2-(4-methoxyphenyl)-*N*-(3-{[2-(4-methoxyphenyl)ethyl]imino}-1,4-dihydro-2-quinoxalinylidene)ethanamine (Fig. 1; see also no. 21 in Fig. S1).

Inhibition of water-insoluble EPS synthesis and Gtf activity. The inhibitory effect of 2-(4-methoxyphenyl)-*N*-(3-{[2-(4-methoxyphenyl)ethyl]imino}-1,4-dihydro-2-quinoxalinylidene) ethanamine on water-insoluble EPS synthesis was evaluated using CLSM. Figure 2A shows representative three-dimensional images of bacteria (green) and EPS (red) in *S. mutans* UA159 biofilms. The vertical distribution of bacteria and EPS from the glass coverslip surface to the liquid interface was calculated using the confocal imaging data sets and COMSTAT (Fig. 2A, below). The data demonstrate that the compound markedly disrupted the ability of *S. mutans* to synthesize the EPS matrix. Consequently, treatment with the compound resulted in reduced biofilm thickness ($P < 0.05$) and a distinct pattern with minimal accumulation of bacterial cells and polysaccharides on the coverslip surfaces. This finding was confirmed by quantitative analyses of the distributions of bacteria and EPS at different time points using CLSM (see Fig. S6A and B in the supplemental material). We used the anthrone-sulfuric acid method to further quantify the amount of water-insoluble EPS (Fig. 2B; see also Fig. S5 in the supplemental material). Figure 2B shows that the compound had a dose-dependent inhibitory effect on *S. mutans* UA159. Notably, there was a >40% reduction in the production of water-insoluble EPS in the 10-μg/ml group compared with that of the control group ($P < 0.05$). We used *gtf* mutant strains to investigate which *S. mutans* Gtfs were inhibited. Our data revealed that the wild-type (WT) (UA159) and the *gtfB* mutant strains showed similar decreases in their ability to synthesize insoluble EPS when treated with the compound. However, the *gtfC* mutant and a *gtfB gtfC* double mutant were not affected by the inhibitor (Fig. 2B). Figure 3 shows representative protein and zymogram patterns of the *S. mutans* Gtfs in the parental and mutant strains. The wild-type strain showed a typical pattern of Gtf activity, with two apparent glucan-synthesized bands, the GtfB at 165.8 kDa, superimposed upon the similarly sized GtfD (163.4 kDa), and the smaller GtfC (153.0 kDa). Enzymatic activities were indicated by the brightness of the corresponding glucan bands. In the WT and Δ*gtfB* strains, GtfC activity was markedly reduced after treatment, confirming that GtfC was targeted by the compound. Interestingly, we found that the glucan bands synthesized by GtfB and GtfD in the Δ*gtfC* strain appeared lighter while the band corresponding to GtfD in the Δ*gtfB* strain appeared darker. We further investigated changes in the level of transcription of *gtfB*, *gtfC*, and *gtfD* in *S. mutans* UA159. Compared with the untreated samples, the expression of *gtfB*, *gtfC*, and *gtfD* in the samples treated with the compound was upregulated 2.9-, 3.3-, and 2.3-fold, respectively (Fig. 2C).

Inhibition of *S. mutans* biofilm formation and maturation. The impact of the compound on the ability of *S. mutans* to form

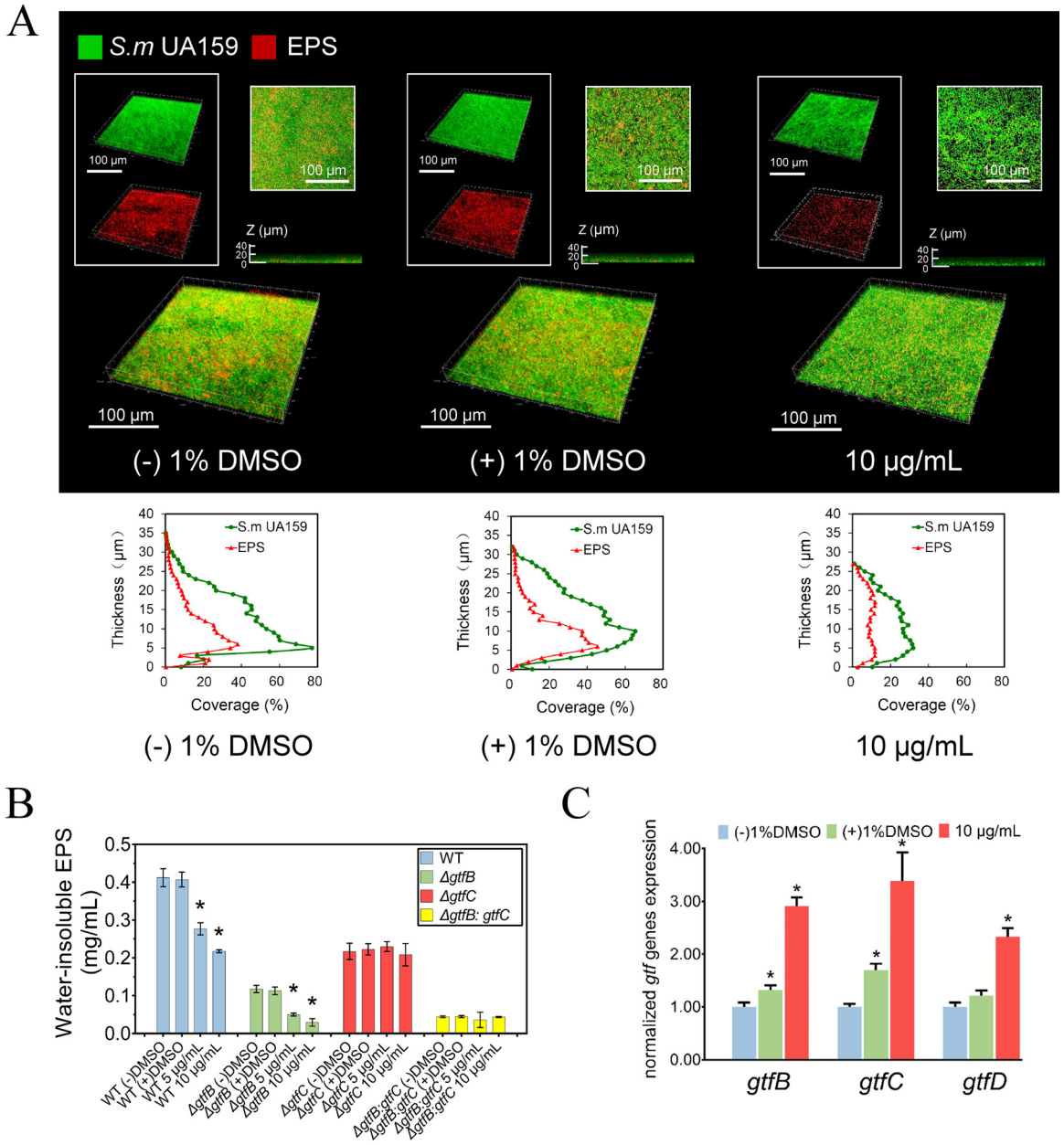

FIG 2 Effect of the compound on the synthesis of polysaccharides in *S. mutans* biofilms. (A) Double-labeling imaging and three-dimensional visualization of EPS (red) and bacteria (green) of an *S. mutans* biofilm formed on the surface of glass coverslip. Images were taken at 60× magnification. Quantitative analysis was performed with COMSTAT, showing the distribution of EPS and bacteria from the coverslip surface to the fluid phase interface. (B) The quantitative data of the water-insoluble polysaccharide amount of *S. mutans* UA159 (WT) and the *gtf* mutants determined colorimetrically by anthrone-sulfuric method. (C) *S. mutans gtf* gene expression determined by quantitative RT-PCR. 16S rRNA was used as an internal control. Values represent the means ± standard deviations from three independent experiments. *, Significant difference compared with the untreated control ($P < 0.05$).

biofilms was investigated by SEM (Fig. 4A). In accord with the previous results related to reductions in glucan synthesis and GTF activity, biofilms treated with 10 μg/ml of the compound showed decreased amounts of exopolysaccharide with a relatively spongy and porous structure compared with those of the control biofilms. Morphologically, the cells did not exhibit an irregular shape, cell wall damage, or swelling, indicating that the compound was not bactericidal. To test whether the compound can affect the viability of *S. mutans* cells within the biofilm, we determined the number of bacterial CFU in the biofilm. The compound decreased the number of viable cells in *S. mutans* biofilms in a concentration-dependent manner (Fig. 4B). In 24-hour-old *S. mutans* biofilms, 5 and 10 μg/ml compound reduced the viable count by 46% and 79%, respectively, compared with that of the negative control ($P < 0.05$). At 0.5 μg/ml or less, no significant antibiofilm effect was detected. At 10 μg/ml, the compound was capable of decreasing the number of viable cells in the biofilms of the *gtfB* and *gtfC* mutant strains. However, the *gtfB gtfC* double mutant strain was not affected by the inhibitor (see Fig. S3 in the supplemental material). Destruction of mature biofilms is a challenging task for

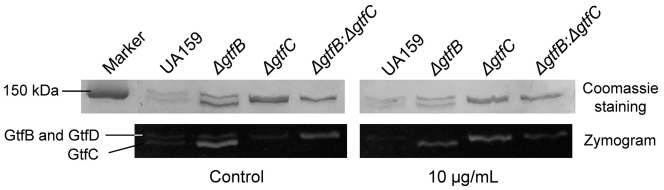

FIG 3 Representative patterns of Gtf isozyme production and activities analyzed by zymogram assays. Gtfs were electrophoretically separated and were analyzed for protein by Coomassie blue staining (above) and for glucan production after incubation of gels with sucrose (bottom), respectively. Strains are indicated above each lane.

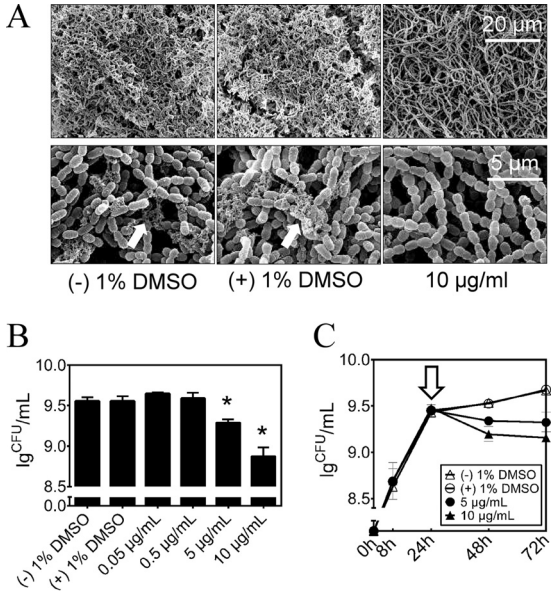

FIG 4 Effect of the compound on the *S. mutans* biofilm formation. (A) Scanning electron microscopy analysis of the architecture of 48-hour biofilms. Images were taken at 5,000× and 20,000× magnification, respectively. Representative images are demonstrated from at least 5 randomly selected positions of each sample. (B) Effect of the treatments on *S. mutans* biofilm formation by determination of the average number of CFU recovered per biofilm. The concentrations of the compound ranged from 0.05 μg/ml to 10 μg/ml. (C) Effect of the compound on mature *S. mutans* biofilms by determination of the average number of CFU recovered per biofilm. Data were collected at 8, 24, 48, and 72 h. Hollow arrow, time of compound challenge.

antimicrobials, as biofilms provide protection for microorganisms against these compounds. In our study, we exposed 24-hour-old *S. mutans* biofilms to the compound for 48 h, and as shown in Fig. 4C, there were clear differences ($P < 0.05$) in the subsequent kinetics of biofilm formation after the single treatment and in a concentration-dependent manner. More interestingly, at 10 μg/ml, the compound reduced the viable cells in *S. sanguinis* biofilms by 85% but did not significantly inhibit *S. gordonii* biofilms (see Fig. S4 in the supplemental material). In the three-species biofilm, the inhibitory profile was similar to those of the monospecies biofilms formed by *S. mutans* and *S. sanguinis* (see Fig. S4). Furthermore, we measured the adhesion properties of *S. mutans* biofilm surfaces at a nanoscale using AFM. The calculated adhesion forces of *S. mutans* biofilms grown in a medium supplemented with the compound are shown in Fig. 5A, and a typical force-distance curve is shown in Fig. 5B. Adhesion forces (mean ± standard deviation [SD]) for *S. mutans* biofilms grown without the compound, in 1% DMSO, or in 5 μg/ml of the compound were found to be 1.7 ± 0.3 nN, 1.0 ± 0.4 nN, and 0.08 ± 0.4 nN, respectively. In the presence of 10 μg/ml of the compound, the adhesion forces were significantly reduced and not detectable (date not shown).

Inhibition of *S. mutans* UA159 virulence and caries formation. The effects of the treatments on the incidence and severity of smooth- and sulcal-surface caries are shown in Table 1. Specifically, treatment with either 10 μg/ml of the compound or 250 μg/ml fluoride significantly reduced the incidence and severity of smooth-surface caries compared with the control groups ($P < 0.05$) (Table 1). However, the group treated with 5 μg/ml of the compound still had significantly fewer severe smooth-surface lesions (at the dentin exposed [Ds] level). Similarly, the incidence and severity of sulcal-surface caries were reduced by either 10 μg/ml of the compound or 250 μg/ml fluoride only. However, treatment with 5 μg/ml of the compound only reduced the severity (at the whole dentin affected [Dx] level) of the lesions ($P < 0.05$). The percentages of *S. mutans* cells recovered from the jaws of the rats were calculated from the total cultivable flora and the *S. mutans* population. The group treated with 10 μg/ml of the compound had a significantly lower level of *S. mutans* infection compared to that of the control group ($P < 0.05$) (Fig. 6A), indicating that it possessed potential selectivity against *S. mutans*. In the animal experiments, all rats remained in apparent good health during the 5-week experiment with no unexpected deaths and with no significant difference in weight gain among the control and experimental groups ($P > 0.05$) (Fig. 6B).

DISCUSSION

In this study, we report the identification of a novel small-molecule compound that inhibits Gtf enzymes of *S. mutans* UA159, thereby inhibiting biofilm formation *in vitro* and *in vivo*. Targeting Gtf enzymes prevents the synthesis of extracellular polysaccharides (EPS) and is an attractive strategy for the development of antibiofilm compounds, as EPS are extremely important in the processes of biofilm formation and stabilization (21). As the capsular-like glucans can protect the microorganisms from inimical influences, such as fluoride and antibiotics, the inhibition of glucan synthesis may enhance the abilities of these agents to reach the microorganisms they are intended to affect, thereby enhancing their biological efficacy. *S. mutans* is the main contributor of these polysaccharides in dental biofilms (22), and GtfC, in particular, has been proven to be one of the most important *S. mutans* virulence factors (24–26). As the structures of the Gtfs are considerably specific for *S. mutans* (43), we expected that a structure-based inhibitor of the *S. mutans* Gtfs would possess narrow-spectrum antibiofilm activity. We investigated the effects of the compound on other oral bacteria and multispecies biofilm formations. Our results supported the idea that the compound had modest selectivity toward the cariogenic bacterium *S. mutans* and one of its commensal colonizers, *S. sanguinis*, but the mechanism behind this is still unclear.

Another advantage of a Gtf-targeted inhibitor is that it is very likely to possess antibiofilm bioactivity without killing the bacterial cells directly, as it has been shown that deletion of *gtfC* only resulted in poor biofilm formation due to reduced adherence rather than to cell death (44). Our results also suggest that the molecule did not inhibit or alter planktonic *S. mutans* growth (see Fig. S2 in the supplemental material). The logarithmic phase was not altered for cells grown in the presence of the compound, and

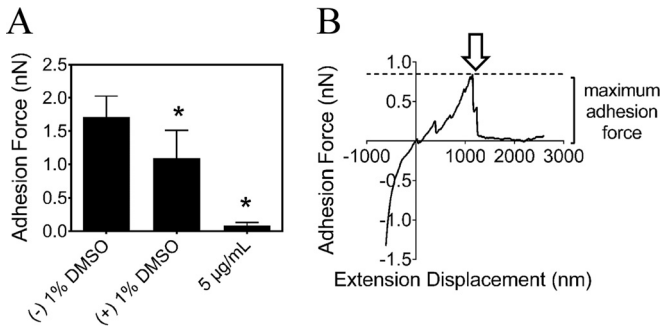

FIG 5 Effect of the compound on the adhesion of *S. mutans* biofilms. (A) Adhesion force characteristics of 24-h *S. mutans* biofilm measured by AFM. All measurements were obtained under PBS (pH 7.2). (B) Illustration of a typical force-distance curve between the AFM tip and the *S. mutans* biofilm. Hollow arrow, time of the final rupture event at a certain length away from the surface. Values represent the means ± standard deviations from three independent experiments. *, Significant difference compared with the untreated control ($P < 0.05$).

we did not observe significant reductions in the final optical density ($P > 0.05$), indicating that the compound is neither bacteriostatic nor bactericidal. This is in accord with recent caries research showing that dental caries is closely associated with cariogenic agents in the form of biofilms rather than planktonic bacteria. Therefore, a reduction in biofilm formation and maturation may be a better strategy to control the formation of caries without disturbing the remaining oral microbiota.

Here, we have discovered, by structure-based virtual screening, a small-molecule compound, 2-(4-methoxyphenyl)-*N*-(3-{[2-(4-methoxyphenyl)ethyl]imino}-1,4-dihydro-2-quinoxalinylidene) ethanamine, which is a novel inhibitor of *S. mutans* Gtfs. A molecular docking study identified the potential binding pocket of the compound in the substrate-binding site of *S. mutans* GtfC, giving insights into the inhibitor's interaction with the enzyme and clues as to how to design new generations of quinoxaline derivatives in the future.

In the present study, we found that the compound not only was able to inhibit the synthesis of water-insoluble extracellular polysaccharides by *S. mutans* UA159 but also caused a significant reduction in the adhesion force of biofilms. The compound exhibited remarkable antibiofilm properties against *S. mutans*, and it is worth noting that suppression of 24-hour-old biofilms was also evident, indicating that the compound can penetrate into the elaborate architecture of the mature biofilm. Interestingly, we observed that the compound also impaired the biofilm formation of the *gtfB* and *gtfC* mutant strains but was ineffective on the *gtfB gtfC* double mutant strain. This phenotypic observation is likely due to the inhibitory effect on GtfB and GtfC, as GtfB is very similar to GtfC in terms of their structural and biological properties (45).

In order to investigate the molecular mechanism underlying these phenotypic responses, we quantitatively analyzed the transcriptions of the glucosyltransferase-encoding genes *gtfB*, *gtfC*, and *gtfD*. Our data showed that along with suppressed EPS synthesis, the compound upregulated the expressions of all three genes to a certain extent, suggesting that *S. mutans* might rally these genes as a means of compensating for the reduced activity of the Gtfs antagonized at the post-translational level. Another possible explanation for this phenomenon is the regulation effect of the quorum-sensing (QS) system of *S. mutans*, which coordinates gene expression according to the population density (46–48). When treated with the inhibitor, decreased cell density due to poor sucrose-dependent adherence might lead to QS regulation that turned on the *gtf* upregulation pathway to enhance cell accumulation in the biofilm. We further identified a reduction in the water-insoluble EPS synthesis of the *gtf* mutants and their parental strain in the presence of the inhibitor. In accord with the results of biofilm formation assays, the compound showed a similar inhibitory effect on the synthesis of water-insoluble EPS in biofilms formed by the WT and Δ*gtfB* strains, while the Δ*gtfC* strain seemed to be more resistant. Furthermore, the cell-free enzyme activities of GtfB, GtfC, and GtfD after treatment with the compound were analyzed directly using zymogram assays, and the data revealed that GtfC together with GtfD was antagonized by the compound. In contrast, we also observed increased GtfB activity in the presence of the compound. Although the exact mechanisms of this phenotypic change are still unclear, these findings suggest that despite the unexpectedly enhanced cell-free GtfB activity, the overall impact of the compound on *S. mutans* biofilms is the negative regulation of extracellular polysaccharide synthesis impairing the formation of a microbial community. We speculate that this may be the primary result of the antagonism of GtfC, which would damage the ability of the cells to adhere and form microcommunities. Besides the sucrose-dependent adherence related to water-insoluble glucans produced from sucrose by Gtfs, the adherence of *S. mutans* to the dental surface is also mediated by sucrose-independent mechanisms (49, 50). For example, the cell-

TABLE 1 Effect of treatments on development of dental caries in rats (Keyes' score)[a]

Treatment	Smooth-surface caries	Smooth-surface severity		Sulcal-surface caries	Sulcal-surface severity (mean [SD])		
		Ds[b]	Dm[c]		Ds	Dm	Dx[d]
Negative control (deionized water)	24.0 (7.9)A	13.2 (6.6)A	2.4 (1.8)A	43.2 (4.6)A	38.6 (2.8)A	21.6 (4.4)A	8.0 (5.1)A
Vehicle control (1% DMSO)	22.8 (6.3)A	16.0 (8.8)A	0.8 (1.3)A	42.6 (7.6)A	41.8 (1.1)A	19.2 (5.8)A	5.0 (5.7)A
Fluoride (250 ppm)	11.0 (4.1)B	2.4 (2.6)B	ND[e]	27.4 (5.7)B	23.0 (4.2)B	7.4 (3.5)BC	ND
Compound (5 μg/ml)	14.2 (5.1)AB	2.8 (1.3)B	ND	39.2 (3.8)AC	34.8 (6.2)A	14.2 (4.1)AC	0.8 (0.8)B
Compound (10 μg/ml)	10.0 (3.9)B	2.4 (2.1)B	ND	30.8 (4.3)BC	22.2 (3.4)B	2.8 (2.7)B	ND

[a] Table values denote means with SD in parentheses ($n = 5$). Values followed by the same letter are not significantly different from each other ($P > 0.05$) (ANOVA; comparison for all pairs using the Tukey-Kramer HSD).
[b] Ds, dentin exposed.
[c] Dm, 3/4 of the dentin affected.
[d] Dx, whole dentin affected.
[e] ND, not detectable.

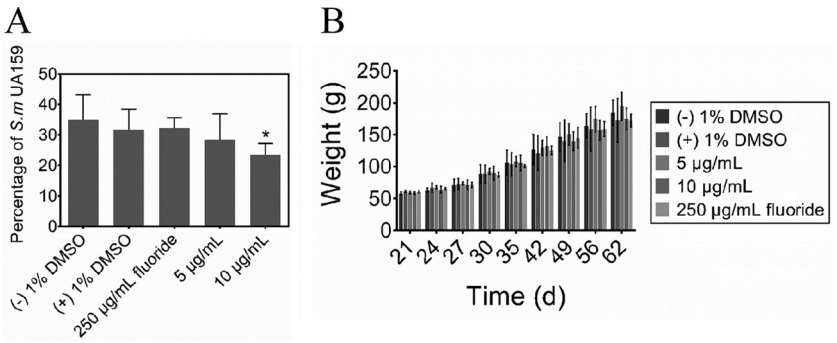

FIG 6 Effects of treatments on percentage of *S. mutans* UA159 and on rat weight gains. (A) Effects of treatments on percentage of *S. mutans* UA159 in rats. (B) Effects of treatments on rat weight gains. Values represent the means ± standard deviations from three independent experiments. *, Significant difference compared with the untreated control ($P < 0.05$).

wall-associated adhesion P1, a member of the antigen I/II family encoded by *spaP*, mediates the adhesion and aggregation of *S. mutans* (51–53). However, it was unlikely that the sucrose-independent adhesion was affected by the inhibitor, as the compound was capable of inhibiting glucan synthesis by Gtfs and the *gtfB gtfC* double mutant strain was not affected in the biofilm formation assays. The data clearly showed that the small-molecule compound exhibited a cariostatic effect on smooth-surface and sulcal-surface caries *in vivo*, with the highest concentration (10 μg/ml) showing an efficacy as potent as fluoride (250 μg/ml), whose anticaries capacity has been clinically proven. Meanwhile, we observed lower levels of *S. mutans* infection in rats treated with the compound compared with those in other groups, indicating that the identified compound was selective against *S. mutans*. These data confirm the findings from the *in vitro* experiments, where the compound exhibited potent antibiofilm activity and supported our hypothesis that we can reduce the incidence and severity of dental caries by inhibiting glucan synthesis by targeting Gtf in *S. mutans*. In addition, we did not observe any adverse reactions in our animals.

A limitation of this study is that it may not represent a complete picture of how the small-molecule inhibitor interacts with the genetic network responsible for biofilm formation, as we tested only the *gtf* genes from *S. mutans*. Since oral biofilms are complex multispecies microbial communities, further research is needed to shed more light on the effect of the compound in real situations. The zymogram assays only measured changes in cell-free Gtf activity, and cell-associated Gtf activity, especially the activity of cell-associated GtfB, might be different. Further research at the molecular level should be done to reveal how the inhibitor interacts with cell-associated Gtfs and how the cell-wall-anchored enzyme activity changes. Furthermore, in order to improve the water solubility of the compound (only 10 μg/ml for the current compound), new quinoxaline derivatives should be designed and synthesized to further enhance their antibiofilm capabilities.

In conclusion, our study has identified a small-molecule compound targeting the glucosyltransferases of *S. mutans* with the capacity to inhibit biofilm formation and cariogenicity and represents an application of structure-based virtual screening in the field of dental research. With its low molecular weight and favorable efficacy *in vitro* and *in vivo*, the compound has the potential to be developed into a preparation for the prevention of dental caries.

ACKNOWLEDGMENTS

We would like to thank Zheng-Guo He of Huazhong Agricultural University for help in molecular docking analysis, Sang-Joon Ahn (of the laboratory of Robert A. Burne at University of Florida, Gainesville, FL) for providing the *gtf* mutant strains, and Jodie Scott for the language revision of the manuscript.

Funding was provided by the National Natural Science Foundation of China under grants 31200985, 81371135, and 31400040, the National Science and Technology Pillar Program during the 12th Five-Year Plan Period under grant 2012BAI07B03, and the State Key Laboratory of Oral Diseases.

The authors declare no potential conflicts of interest with respect to the authorship and/or publication of this article.

FUNDING INFORMATION

National Science and Technology Pillar Program during the 12th Five Year Plan Period provided funding to Jiyao Li under grant number 2012BAI07B03. State Key Laboratory of Oral Diseases provided funding to Yuqing Li under grant number SKLOD201414. National Natural Science Foundation of China provided funding to Yuqing Li under grant number 31200985. National Natural Science Foundation of China (NSFC) provided funding to Jumei Zeng under grant number 31400040. National Natural Science Foundation of China (NSFC) provided funding to Jiyao Li under grant number 81371135.

REFERENCES

1. **Petersen PE, Kwan S.** 2009. World Health Organization global oral health strategies for oral health promotion and disease prevention in the twenty-first century. Präv Gesundheitsf **4:**100–104.
2. **Marchisio O, Esposito M, Genovesi A.** 2010. Salivary pH level and bacterial plaque evaluation in orthodontic patients treated with Recaldent products. Int J Dent Hyg **8:**232–236.
3. **Söder B, Yakob M, Meurman JH, Andersson LC, Söder P-Ö.** 2012. The association of dental plaque with cancer mortality in Sweden. A longitudinal study. BMJ Open **2:**e001083.
4. **Tanzer JM, Livingston J, Thompson AM.** 2001. The microbiology of primary dental caries in humans. J Dent Educ **65:**1028–1037.
5. **Keene HJ, Shklair IL.** 1974. Relationship of *Streptococcus mutans* carrier status to the development of carious lesions in initially caries-free recruits. J Dent Res **53:**1295. http://dx.doi.org/10.1177/00220345740530053801.
6. **He X, Lux R, Kuramitsu HK, Anderson MH, Shi W.** 2009. Achieving probiotic effects via modulating oral microbial ecology. Adv Dent Res **21:**53–56. http://dx.doi.org/10.1177/0895937409335626.
7. **Marsh PD.** 2010. Microbiology of dental plaque biofilms and their role in oral health and caries. Dent Clin North Am **54:**441–454. http://dx.doi.org/10.1016/j.cden.2010.03.002.
8. **Becker MR, Paster BJ, Leys EJ, Moeschberger ML, Kenyon SG, Galvin JL, Boches SK, Dewhirst FE, Griffen AL.** 2002. Molecular analysis of

bacterial species associated with childhood caries. J Clin Microbiol **40:** 1001–1009. http://dx.doi.org/10.1128/JCM.40.3.1001-1009.2002.

9. **Koo H, Duarte S, Murata R, Scott-Anne K, Gregoire S, Watson G, Singh A, Vorsa N.** 2010. Influence of cranberry proanthocyanidins on formation of biofilms by *Streptococcus mutans* on saliva-coated apatitic surface and on dental caries development *in vivo*. Caries Res **44:**116–126. http://dx.doi.org/10.1159/000296306.
10. **Stauder M, Papetti A, Daglia M, Vezzulli L, Gazzani G, Varaldo PE, Pruzzo C.** 2010. Inhibitory activity by barley coffee components towards *Streptococcus mutans* biofilm. Curr Microbiol **61:**417–421. http://dx.doi.org/10.1007/s00284-010-9630-5.
11. **Xu X, Zhou XD, Wu CD.** 2012. Tea catechin epigallocatechin gallate inhibits *Streptococcus mutans* biofilm formation by suppressing *gtf* genes. Arch Oral Biol **57:**678–683. http://dx.doi.org/10.1016/j.archoralbio.2011.10.021.
12. **Koo H, Pearson S, Scott-Anne K, Abranches J, Cury J, Rosalen P, Park Y, Marquis R, Bowen W.** 2002. Effects of apigenin and *tt*-farnesol on glucosyltransferase activity, biofilm viability and caries development in rats. Oral Microbiol Immunol **17:**337–343. http://dx.doi.org/10.1034/j.1399-302X.2002.170602.x.
13. **Murata RM, Branco-de-Almeida LS, Franco EM, Yatsuda R, dos Santos MH, de Alencar SM, Koo H, Rosalen PL.** 2010. Inhibition of *Streptococcus mutans* biofilm accumulation and development of dental caries *in vivo* by 7-epiclusianone and fluoride. Biofouling **26:**865–872. http://dx.doi.org/10.1080/08927014.2010.527435.
14. **Koo H, Hayacibara M, Schobel B, Cury J, Rosalen P, Park Y, Vacca-Smith A, Bowen W.** 2003. Inhibition of *Streptococcus mutans* biofilm accumulation and polysaccharide production by apigenin and *tt*-farnesol. J Antimicrob Chemother **52:**782–789. http://dx.doi.org/10.1093/jac/dkg449.
15. **Fontana M, González-Cabezas C.** 2012. Are we ready for definitive clinical guidelines on xylitol/polyol use? Adv Dent Res **24:**123–128. http://dx.doi.org/10.1177/0022034512449468.
16. **Twetman S, Keller M.** 2012. Probiotics for caries prevention and control. Adv Dent Res **24:**98–102. http://dx.doi.org/10.1177/0022034512449465.
17. **Kraivaphan P, Amornchat C, Triratana T, Mateo L, Ellwood R, Cummins D, DeVizio W, Zhang Y.** 2013. Two-year caries clinical study of the efficacy of novel dentifrices containing 1.5% arginine, an insoluble calcium compound, and 1,450 ppm fluoride. Caries Res **47:**582–590. http://dx.doi.org/10.1159/000353183.
18. **Li L, Guo L, Lux R, Eckert R, Yarbrough D, He J, Anderson M, Shi W.** 2010. Targeted antimicrobial therapy against *Streptococcus mutans* establishes protective non-cariogenic oral biofilms and reduces subsequent infection. Int J Oral Sci **2:**66–73. http://dx.doi.org/10.4248/IJOS10024.
19. **Kaplan CW, Sim JH, Shah KR, Kolesnikova-Kaplan A, Shi W, Eckert R.** 2011. Selective membrane disruption: mode of action of C16G2, a specifically targeted antimicrobial peptide. Antimicrob Agents Chemother **55:**3446–3452. http://dx.doi.org/10.1128/AAC.00342-11.
20. **Liu C, Worthington RJ, Melander C, Wu H.** 2011. A new small molecule specifically inhibits the cariogenic bacterium *Streptococcus mutans* in multispecies biofilms. Antimicrob Agents Chemother **55:**2679–2687. http://dx.doi.org/10.1128/AAC.01496-10.
21. **Branda SS, Vik S, Friedman L, Kolter R.** 2005. Biofilms: the matrix revisited. Trends Microbiol **13:**20–26. http://dx.doi.org/10.1016/j.tim.2004.11.006.
22. **Tamesada M, Kawabata S, Fujiwara T, Hamada S.** 2004. Synergistic effects of streptococcal glucosyltransferases on adhesive biofilm formation. J Dent Res **83:**874–879. http://dx.doi.org/10.1177/154405910408301110.
23. **Kuramitsu HK.** 2003. Molecular genetic analysis of the virulence of oral bacterial pathogens: an historical perspective. Crit Rev Oral Biol Med **14:**331–344. http://dx.doi.org/10.1177/154411130301400504.
24. **Tanzer J, Freedman M, Fitzgerald R.** 1985. Virulence of mutants defective in glucosyltransferase, dextran-mediated aggregation, or dextranase activity, p 204–211. *In* Mergenhagen SE, Rosan B (ed), Molecular basis of oral microbial adhesion. American Society for Microbiology, Washington, DC.
25. **Munro C, Michalek SM, Macrina FL.** 1991. Cariogenicity of *Streptococcus mutans* V403 glucosyltransferase and fructosyltransferase mutants constructed by allelic exchange. Infect Immun **59:**2316–2323.
26. **Yamashita Y, Bowen W, Burne R, Kuramitsu H.** 1993. Role of the *Streptococcus mutans gtf* genes in caries induction in the specific-pathogen-free rat model. Infect Immun **61:**3811–3817.
27. **Ito K, Ito S, Shimamura T, Weyand S, Kawarasaki Y, Misaka T, Abe K, Kobayashi T, Cameron AD, Iwata S.** 2011. Crystal structure of glucansucrase from the dental caries pathogen *Streptococcus mutans*. J Mol Biol **408:**177–186. http://dx.doi.org/10.1016/j.jmb.2011.02.028.
28. **Ewing TJ, Makino S, Skillman AG, Kuntz ID.** 2001. DOCK 4.0: search strategies for automated molecular docking of flexible molecule databases. J Comput Aided Mol Des **15:**411–428. http://dx.doi.org/10.1023/A:1011115820450.
29. **Irwin JJ, Shoichet BK.** 2005. ZINC—a free database of commercially available compounds for virtual screening. J Chem Inf Model **45:**177–182. http://dx.doi.org/10.1021/ci049714+.
30. **Rose PW, Bi C, Bluhm WF, Christie CH, Dimitropoulos D, Dutta S, Green RK, Goodsell DS, Prlić A, Quesada M, Quinn GB, Ramos AG, Westbrook JD, Young J, Zardecki C, Berman HM, Bourne PE.** 2013. The RCSB Protein Data Bank: new resources for research and education. Nucleic Acids Res **41:**D475–D482. http://dx.doi.org/10.1093/nar/gks1200.
31. **Pettersen EF, Goddard TD, Huang CC, Couch GS, Greenblatt DM, Meng EC, Ferrin TE.** 2004. UCSF Chimera—a visualization system for exploratory research and analysis. J Comput Chem **25:**1605–1612. http://dx.doi.org/10.1002/jcc.20084.
32. **Laskowski RA, Swindells MB.** 2011. LigPlot+: multiple ligand-protein interaction diagrams for drug discovery. J Chem Infect Model **51:**2778–2786. http://dx.doi.org/10.1021/ci200227u.
33. **Ahn S-J, Ahn S-J, Wen ZT, Brady LJ, Burne RA.** 2008. Characteristics of biofilm formation by *Streptococcus mutans* in the presence of saliva. Infect Immun **76:**4259–4268. http://dx.doi.org/10.1128/IAI.00422-08.
34. **Stepanovic S, Vukovic D, Dakic I, Savic B, Svabic-Vlahovic M.** 2000. A modified microtiter-plate test for quantification of staphylococcal biofilm formation. J Microbiol Methods **40:**175–179. http://dx.doi.org/10.1016/S0167-7012(00)00122-6.
35. **Klein M, Duarte S, Xiao J, Mitra S, Foster T, Koo H.** 2009. Structural and molecular basis of the role of starch and sucrose in *Streptococcus mutans* biofilm development. Appl Environ Microbiol **75:**837–841. http://dx.doi.org/10.1128/AEM.01299-08.
36. **Heydorn A, Nielsen AT, Hentzer M, Sternberg C, Givskov M, Ersbøll BK, Molin S.** 2000. Quantification of biofilm structures by the novel computer program COMSTAT. Microbiology **146:**2395–2407. http://dx.doi.org/10.1099/00221287-146-10-2395.
37. **Sharma S, Lavender S, Woo J, Guo L, Shi W, Kilpatrick-Liverman L, Gimzewski JK.** 2014. Nanoscale characterization of effect of L-arginine on *Streptococcus mutans* biofilm adhesion by atomic force microscopy. Microbiology **160:**1466–1473. http://dx.doi.org/10.1099/mic.0.075267-0.
38. **Mattos-Graner RO, Napimoga MH, Fukushima K, Duncan MJ, Smith DJ.** 2004. Comparative analysis of Gtf isozyme production and diversity in isolates of *Streptococcus mutans* with different biofilm growth phenotypes. J Clin Microbiol **42:**4586–4592. http://dx.doi.org/10.1128/JCM.42.10.4586-4592.2004.
39. **Xu X, Zhou XD, Wu CD.** 2011. The tea catechin epigallocatechin gallate suppresses cariogenic virulence factors of *Streptococcus mutans*. Antimicrob Agents Chemother **55:**1229–1236. http://dx.doi.org/10.1128/AAC.01016-10.
40. **Bowen W, Madison K, Pearson S.** 1988. Influence of desalivation in rats on incidence of caries in intact cagemates. J Dent Res **67:**1316–1318. http://dx.doi.org/10.1177/00220345880670101401.
41. **Yanagida A, Kanda T, Tanabe M, Matsudaira F, Oliveira Cordeiro JG.** 2000. Inhibitory effects of apple polyphenols and related compounds on cariogenic factors of mutans streptococci. J Agric Food Chem **48:**5666–5671. http://dx.doi.org/10.1021/jf000363i.
42. **Larson R.** 1981. Merits and modifications of scoring rat dental caries by Keyes' method, p 195–203. *In* Tanzer J (ed), Animal models in cariology. IRL Press, Washington, DC.
43. **Hoshino T, Fujiwara T, Kawabata S.** 2012. Evolution of cariogenic character in *Streptococcus mutans*: horizontal transmission of glycosyl hydrolase family 70 genes. Sci Rep **2:**518.
44. **Koo H, Xiao J, Klein M, Jeon J.** 2010. Exopolysaccharides produced by *Streptococcus mutans* glucosyltransferases modulate the establishment of microcolonies within multispecies biofilms. J Bacteriol **192:**3024–3032. http://dx.doi.org/10.1128/JB.01649-09.
45. **Fukushima K, Okada T, Ochiai K.** 1993. Production, characterization, and application of monoclonal antibodies which distinguish three glucosyltransferases from *Streptococcus mutans*. Infect Immun **61:**323–328.
46. **Smith E, Spatafora G.** 2012. Gene regulation in *S. mutans*: complex control in a complex environment. J Dent Res **91:**133–141.

47. **Ahn S-J, Wen ZT, Burne RA.** 2006. Multilevel control of competence development and stress tolerance in *Streptococcus mutans* UA159. Infect Immun **74:**1631–1642. http://dx.doi.org/10.1128/IAI.74.3.1631-1642.2006.
48. **Li YH, Tang N, Aspiras MB, Lau PC, Lee JH, Ellen RP, Cvitkovitch DG.** 2002. A quorum-sensing signaling system essential for genetic competence in *Streptococcus mutans* is involved in biofilm formation. J Bacteriol **184:**2699–2708. http://dx.doi.org/10.1128/JB.184.10.2699-2708.2002.
49. **Koga T, Asakawa H, Okahashi N, Hamada S.** 1986. Sucrose-dependent cell adherence and cariogenicity of serotype c *Streptococcus mutans*. J Gen Microbiol **132:**2873–2883.
50. **Cvitkovitch DG, Li Y-H, Ellen RP.** 2003. Quorum sensing and biofilm formation in streptococcal infections. J Clin Invest **112:**1626–1632. http://dx.doi.org/10.1172/JCI200320430.
51. **Lee S, Progulske-Fox A, Erdos G, Piacentini D, Ayakawa G, Crowley P, Bleiweis A.** 1989. Construction and characterization of isogenic mutants of *Streptococcus mutans* deficient in major surface protein antigen P1 (I/II). Infect Immun **57:**3306–3313.
52. **Jenkinson HF, Demuth DR.** 1997. Structure, function and immunogenicity of streptococcal antigen I/II polypeptides. Mol Microbiol **23:**183–190. http://dx.doi.org/10.1046/j.1365-2958.1997.2021577.x.
53. **Brady LJ, Piacentini DA, Crowley PJ, Oyston P, Bleiweis AS.** 1992. Differentiation of salivary agglutinin-mediated adherence and aggregation of mutans streptococci by use of monoclonal antibodies against the major surface adhesin P1. Infect Immun **60:**1008–1017.